Supporting Information

Selective Adsorptive Separation of Cyclohexane Over Benzene by Thienothiophene Cages

Yanjun Ding,[a] Lukman O. Alimi,[a] Basem Moosa,[a] Carine Maaliki,[b] Johan Jacquemin,[b] Feihe Huang[c] and Niveen M. Khashab*[a]

[a] Smart Hybrid Materials (SHMs) Laboratory, Advanced Membranes and Porous Materials Center, King Abdullah University of Science and Technology (KAUST), Thuwal 23955-6900, Kingdom of Saudi Arabia.

[b] Laboratoire PCM2E, Université de Tours, Parc de Grandmont, 37200 Tours, France.

[c] State Key Laboratory of Chemical Engineering, Center for Chemistry of High-Performance & Novel Materials, Department of Chemistry, Zhejiang University, Hangzhou 310027, P. R. China

Experimental Procedures

Materials. All chemicals, including benzene (Bz) and cyclohexane (Cy), were purchased from commercial sources and used as received.

Synthesis of Thienothiophene Cages. Tren (292.48 mg; 2.0 mmol) was dissolved in MeCN (5 mL), then thieno[2,3-b]thiophene-2,5-dicarboxaldehyde (588.75 mg; 3.0 mmol) in MeCN (50 mL) was added dropwise over 1 h. The reaction mixture was stirred overnight at room temperature. A light-yellow precipitate was formed which was filtered and washed further with MeCN, then dissolved in dichloromethane and filtered to remove polymers. After the removal of dichloromethane, ThT-cage was obtained in 70% yield. ^{1}H NMR (400 MHz, $CDCl_3$): δ 8.28 (s, 1H), 6.49 (s, 1H), 3.76 (t, J = 4.9 Hz, 2H), 2.78 (s, 2H); ^{13}C NMR (101 MHz, $CDCl_3$) δ 157.73, 146.05, 144.95, 141.37, 125.47, 56.04, 53.08. HRMS (ESI) calcd for $C_{36}H_{37}N_8S_6$ [$(M+H)^+$]: 773.1465, Found: 773.1391.

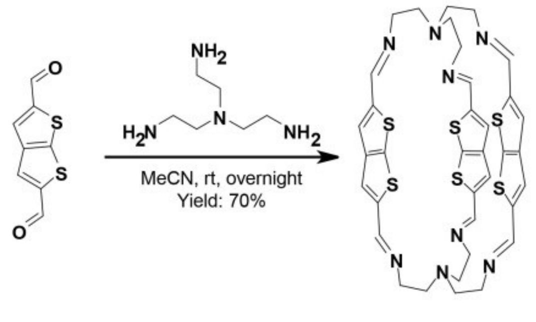

Scheme S1. Synthethic scheme of the ThT-cage.

Single Crystal Growth. Single crystals of **ThT-cage 1** were obtained by liquid diffusion of hexane into a chloroform solution at room temperature; Single crystals of **ThT-cage 2** were grown by slow cooling of a hot benzene solution to room temperature; Single crystals of **ThT-cage 3** were obtained by liquid diffusion of cyclohexane into a chloroform solution at room temperature. All three crystals are colorless.

Adsorption Material Activation. Single crystals of **ThT-cage 1** were dried under vacuum at 80 ^{o}C for 24 h to obtain the **ThT-cage 1α**. While the **ThT-cage 1α** after adsorption was regenerated to release the adsorbed guests upon heating at 100 ^{o}C under vacuum overnight.

Adsorption Experiments for Bz or Cy vapor. An open 5 mL vial containing 10 mg of the activated **ThT-cage 1α** adsorbent was placed in a sealed 20 mL vial containing 1 mL of solvents (Bz, Cy or an equimolar Bz/Cy mixture).

Single X-ray Crystal Structure Determination

Single crystal X-ray diffraction data were recorded on a Bruker D8 Venture equipped with a digital camera diffractometer using graphite-monochromated Cu Kα radiation (λ= 1.54178 Å) for the crystal structure. Data reductions were carried out by means of a standard procedure using the Bruker software package SaintPlus 6.01.[1] The absorption corrections and the correction of other systematic errors were performed using SADABS.[2] The structures were solved by direct methods using SHELXS-2008 and refined using SHELXL-2018.[3] X-Seed[4] was used as the graphical interface for the SHELX program suite. Data collection, structure refinement parameters and crystallographic data for the crystals are given in **Table S1**.

Characterization

Powder X-ray diffraction (PXRD) patterns were obtained using a D8 ADVANCE Twin X-ray diffractometer (40 Kv, 40 mA) with Cu Kα radiation (λ = 1.54178 Å). Data were measured over the range of 3−45° in 1.2°/min steps. NMR spectra were recorded on Bruker-400 (400 MHz for ^{1}H; 101 MHz for ^{13}C) instruments internally referenced to $SiMe_4$ signal. Low-pressure gas adsorption measurement was performed on a Micrometritics Accelerated Surface Area and Porosimetry System (ASAP) 2020 surface area analyzer. Samples were degassed under dynamic vacuum for 12 h at 60 °C prior to each measurement. N_2 isotherms were measured using a liquid nitrogen bath (77 K). Thermogravimetric analysis (TGA) was carried out using a TGA Q50 analyzer (TA Instruments) with an automated vertical overhead thermobalance. The samples were heated at 10 °C/min from 25 to 800 ^{o}C using N_2 as the protective gas. Gas

Chromatographic (GC) Analysis: GC measurements were carried out using a J&W (122-1364) instrument configured with an FID detector and a DB-624 column (60 m × 0.25 mm × 1.4 μm). The following GC method was used: the oven was programmed from 40 °C ramped in 10 °C/min increments to 240 °C with 26 min hold; the total run time was 50 min; the injection temperature was 250 °C; the detector temperature was 260 °C with hydrogen, air, and make-up flow rates of 35, 350, and 30 mL/min, respectively; the helium (carrier gas) flow rate was 3.0 mL/min. The samples were injected in the splitless mode.

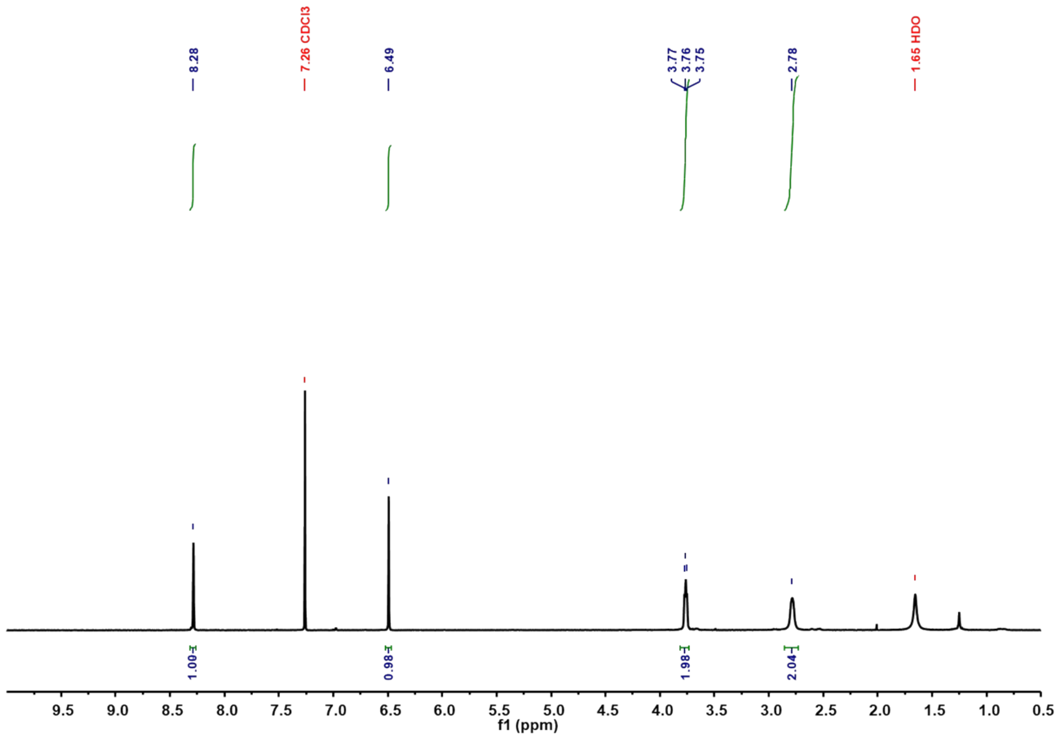

Fig. S1 ^1H NMR spectrum (400 MHz, 298K, $CDCl_3$) of **ThT-cage** (HDO peak comes from trace amount of water in $CDCl_3$).

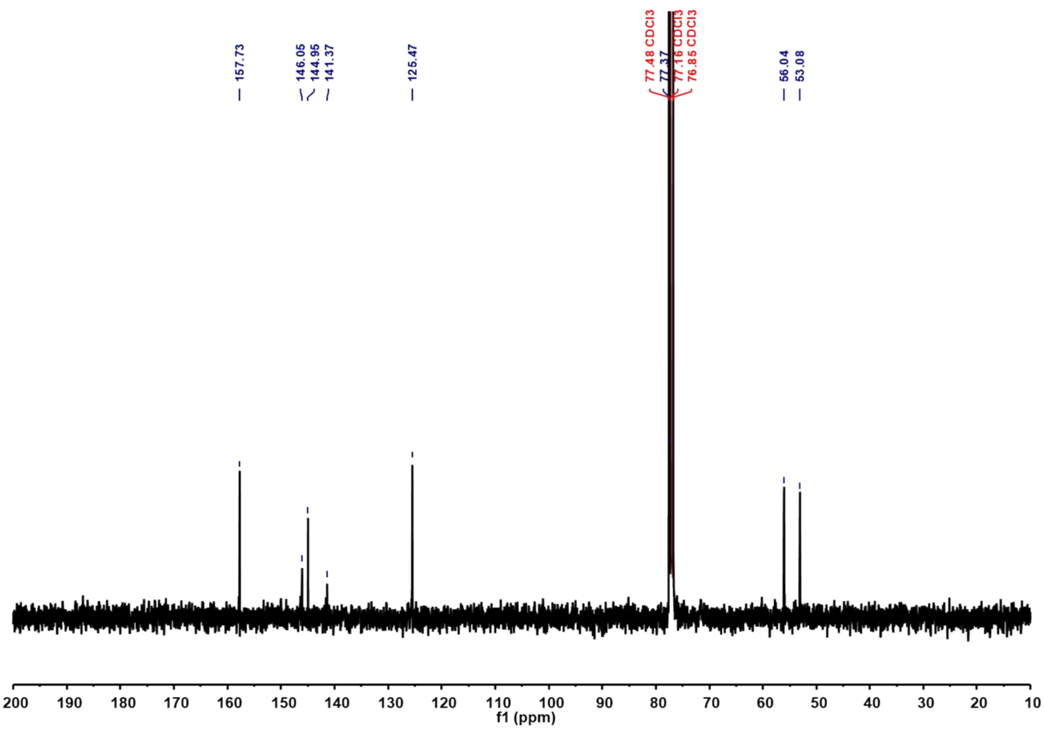

Fig. S2 ^{13}C NMR spectrum (101 MHz, 298K, $CDCl_3$) of **ThT-cage**.

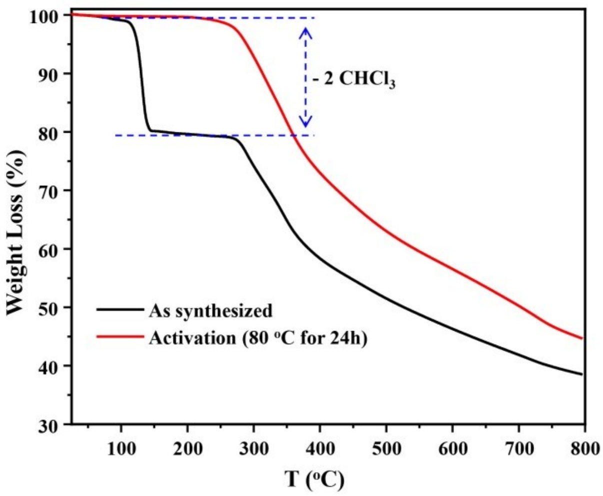

Fig. S3 Thermogravimetric analysis of the as synthesized crystals (**ThT-cage 1**) and the activated ones.

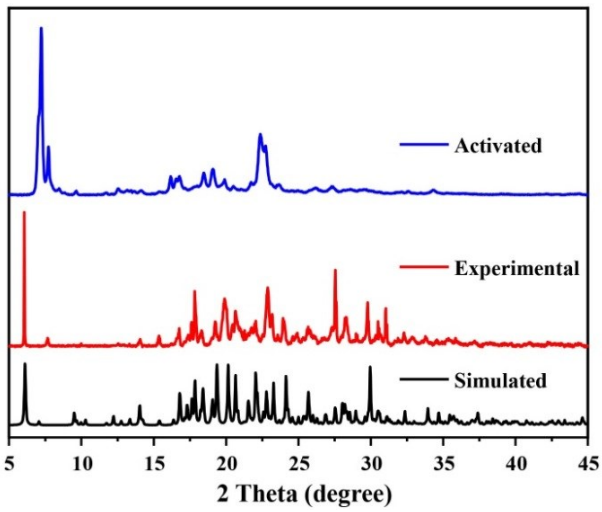

Fig. S4 The PXRD spectra of the as synthesized crystals (**ThT-cage 1**) and the corresponding simulated and activated ones.

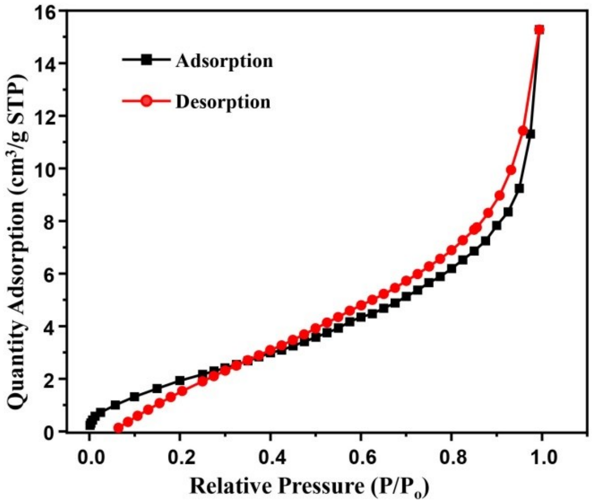

Fig. S5 Nitrogen adsorption isotherm at 77 K for the **ThT-cage 1α.**

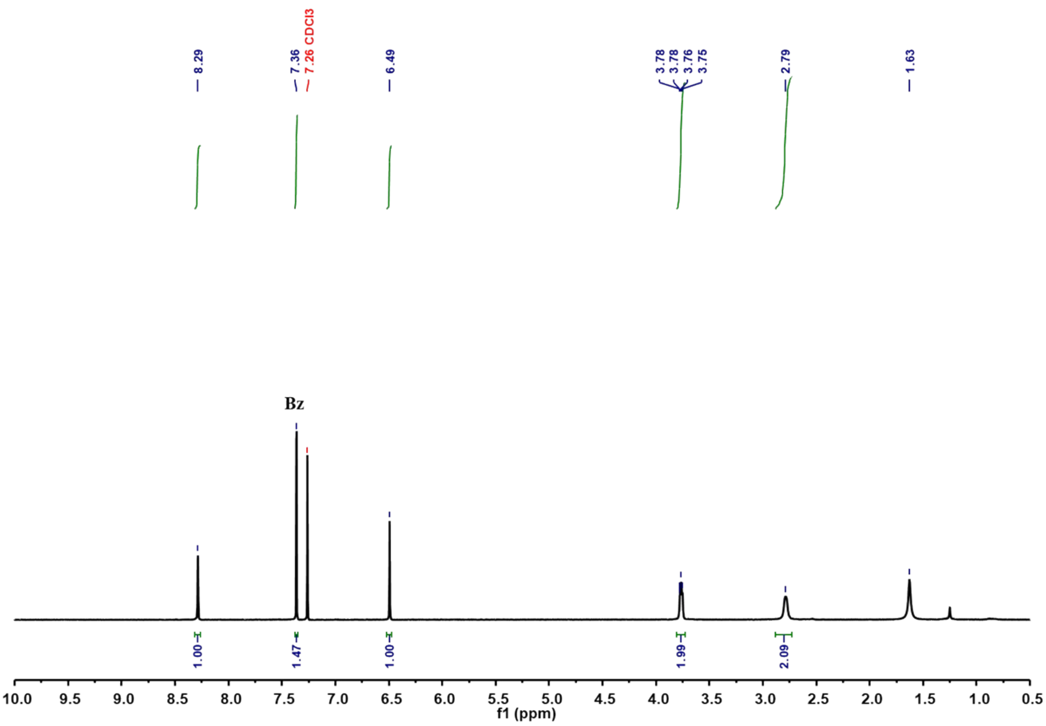

Fig. S6 ^{1}H NMR spectrum (400 MHz, 298K, $CDCl_3$) of the **ThT-cage 1α** after being exposed to Bz for 24 h.

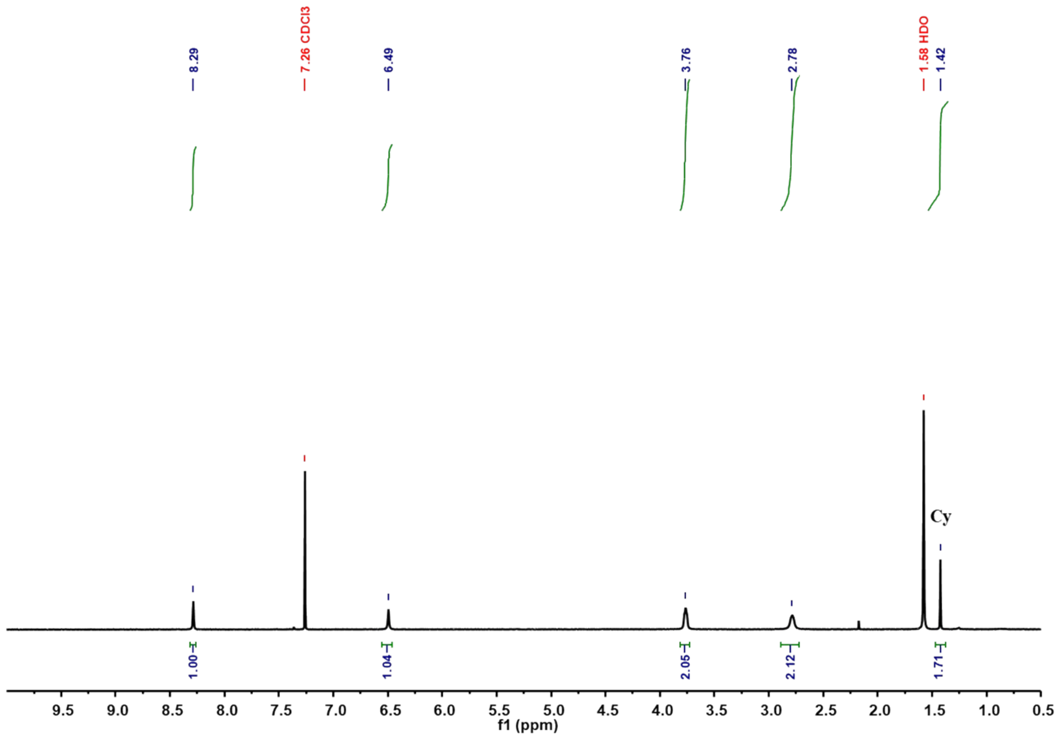

Fig. S7 ^{1}H NMR spectrum (400 MHz, 298K, $CDCl_3$) of the **ThT-cage 1α** after being exposed to Cy for 24 h (HDO peak comes from trace amount of water in $CDCl_3$).

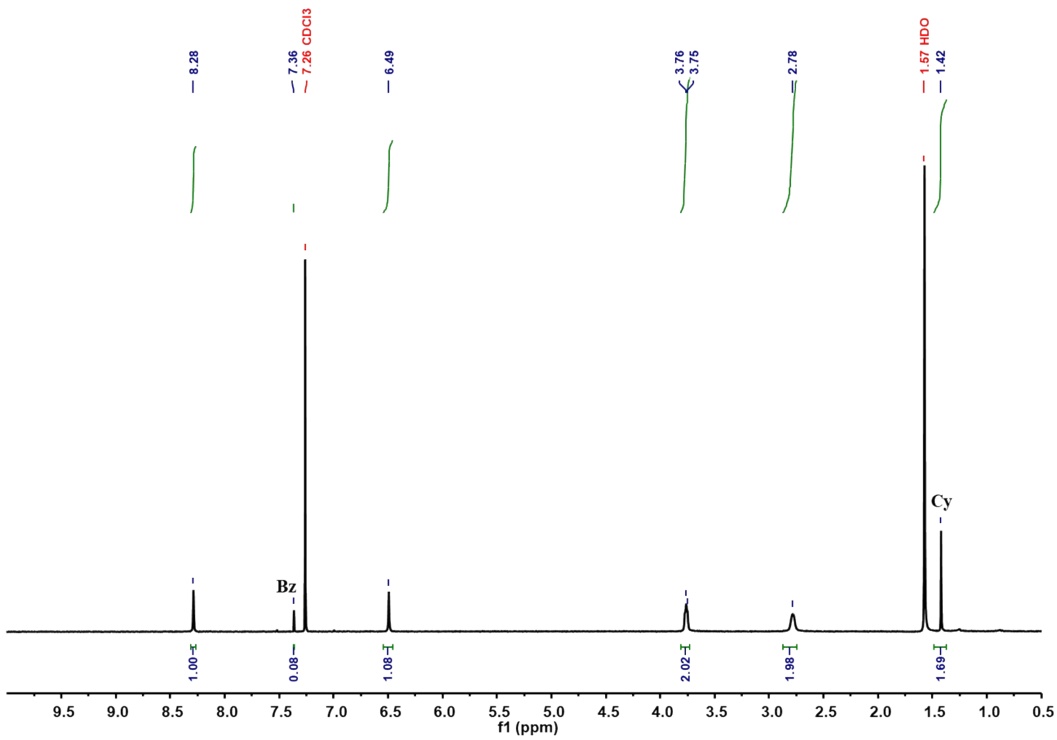

Fig. S8 ^{1}H NMR spectrum (400 MHz, 298K, $CDCl_3$) of the **ThT-cage 1α** after being exposed to Bz/Cy equimolar mixture for 24 h (HDO peak comes from trace amount of water in $CDCl_3$).

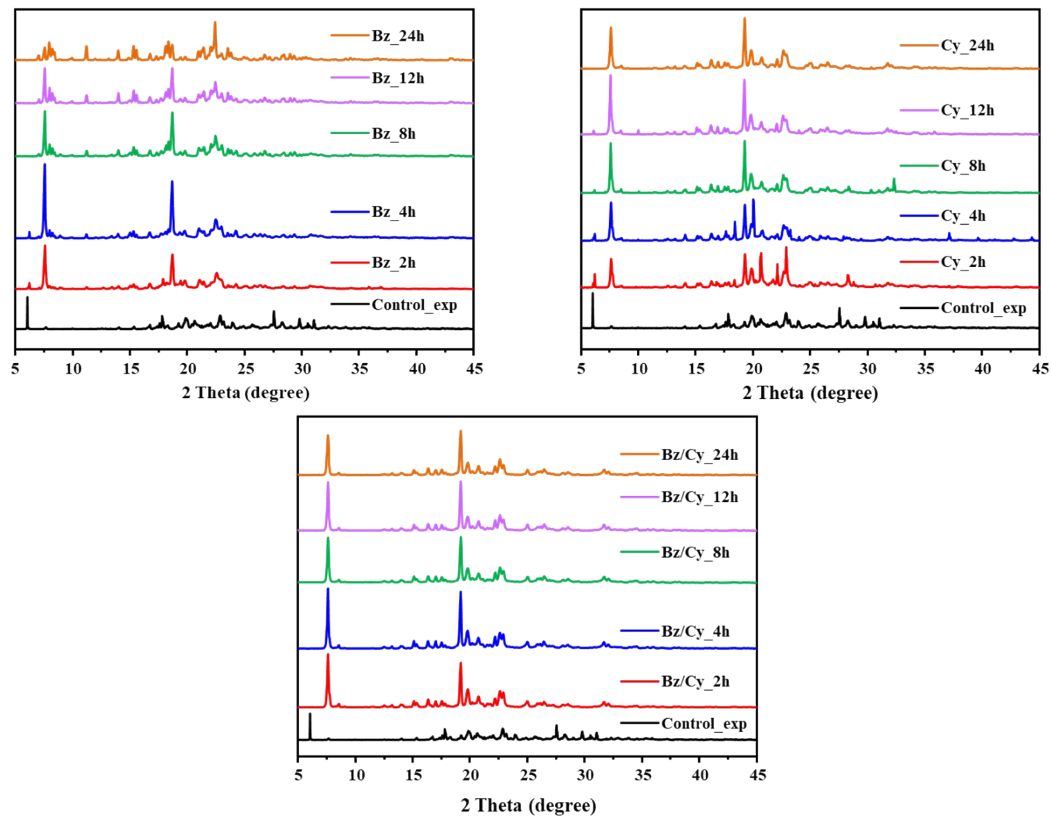

Fig. S9 Experimental PXRD patterns showing the structure conversion after **ThT-cage 1α** being exposed to Bz, Cy and Bz/Cy mixture under different times, respectively.

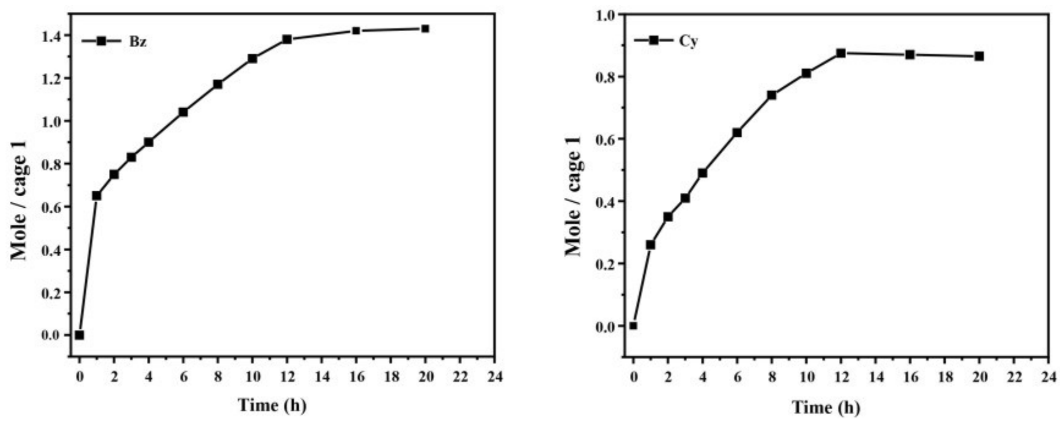

Fig. S10 Time-dependent solid−vapor sorption plots of the **ThT-cage 1α** for single-component Bz and Cy vapor, respectively.

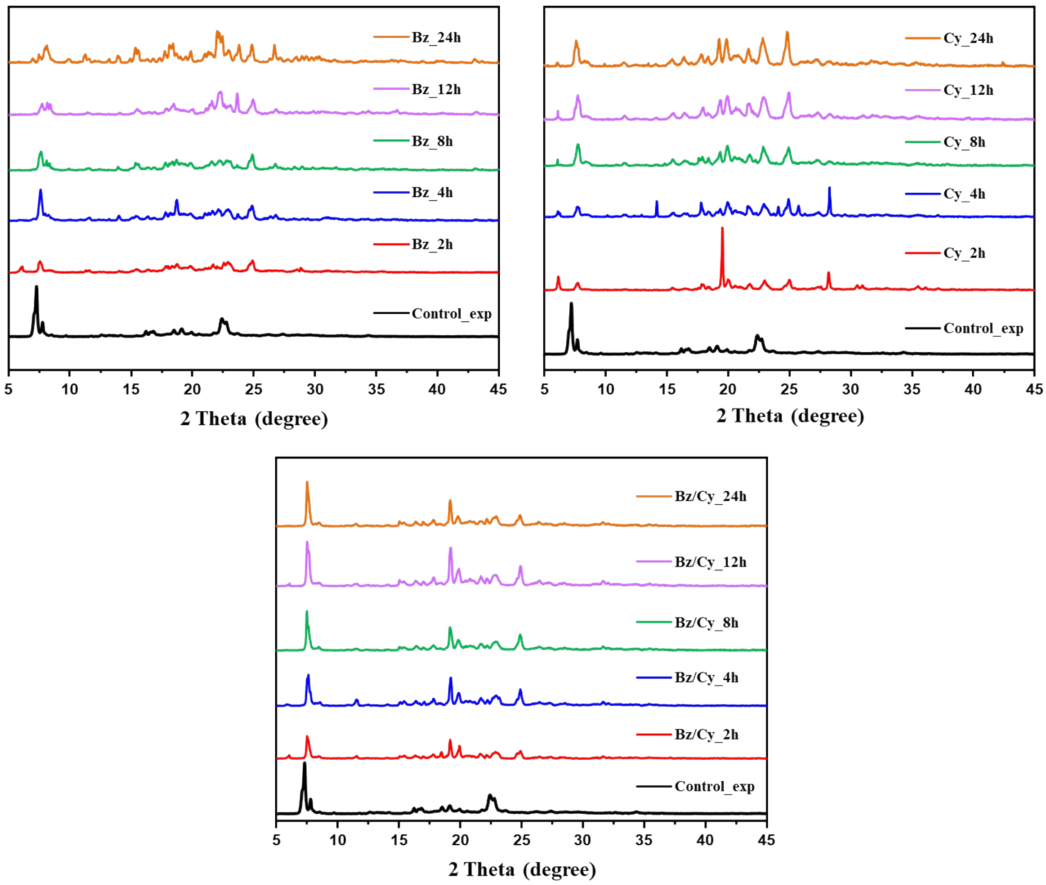

Fig. S11 Experimental PXRD patterns of the solid-liquid sorption experiments.

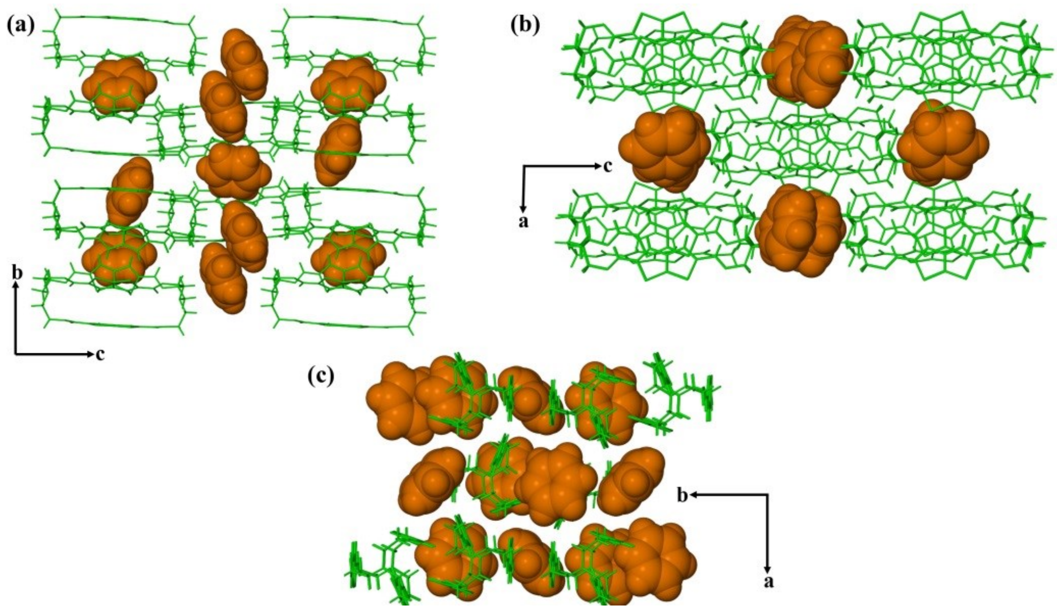

Fig. S12 Single-crystal structure of **ThT-cage 2** from different views (a-c).

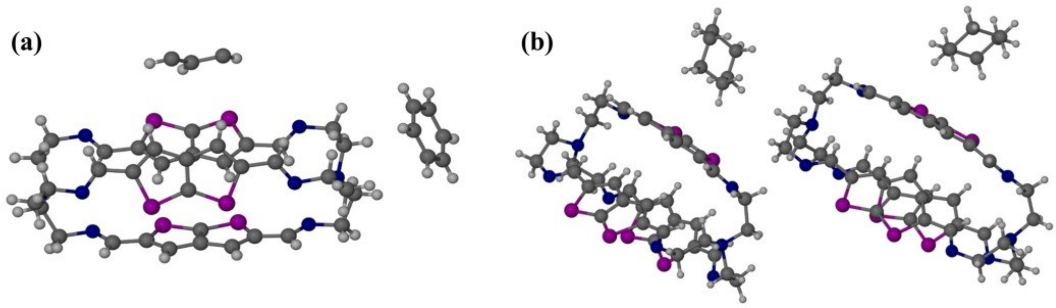

Fig. S13 The asymmetric unit of crystals (a) **ThT-cage 2** and (b) **ThT-cage 3**.

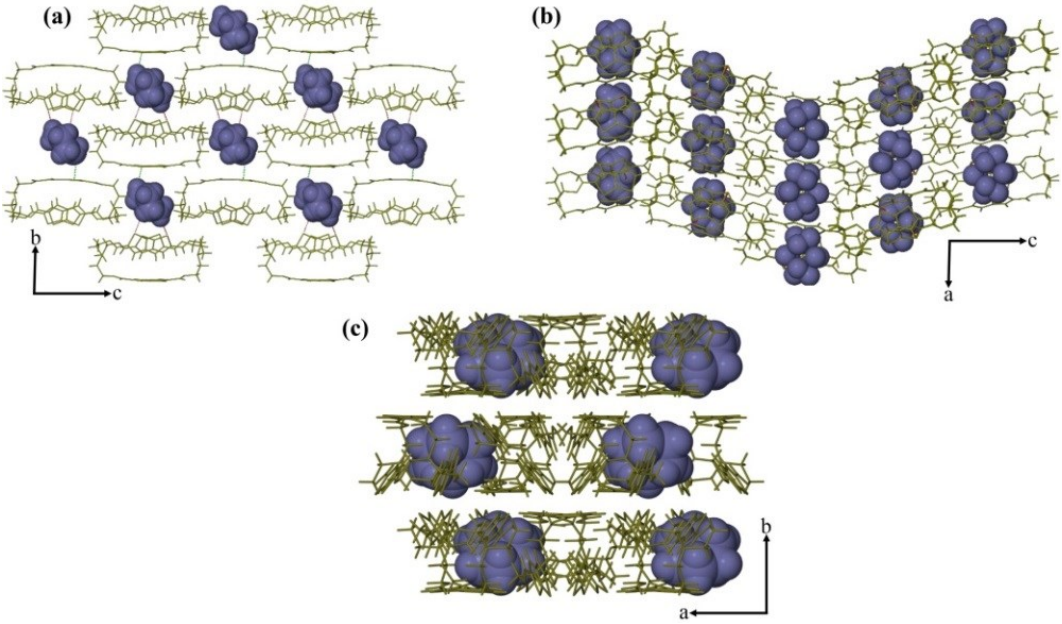

Fig. S14 Single-crystal structure of **ThT-cage 3** from different views (a-c).

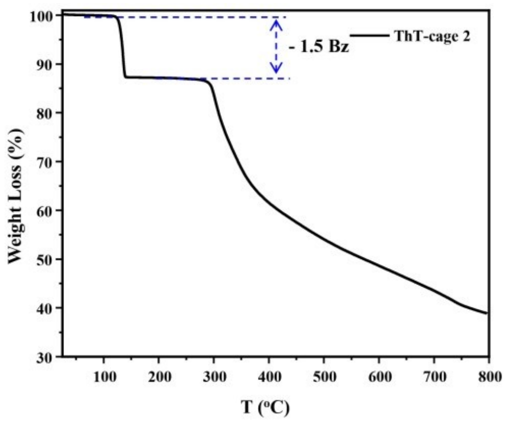

Fig. S15 Thermogravimetric analysis of the as synthesized crystals **ThT-cage 2** and **ThT-cage 3**.

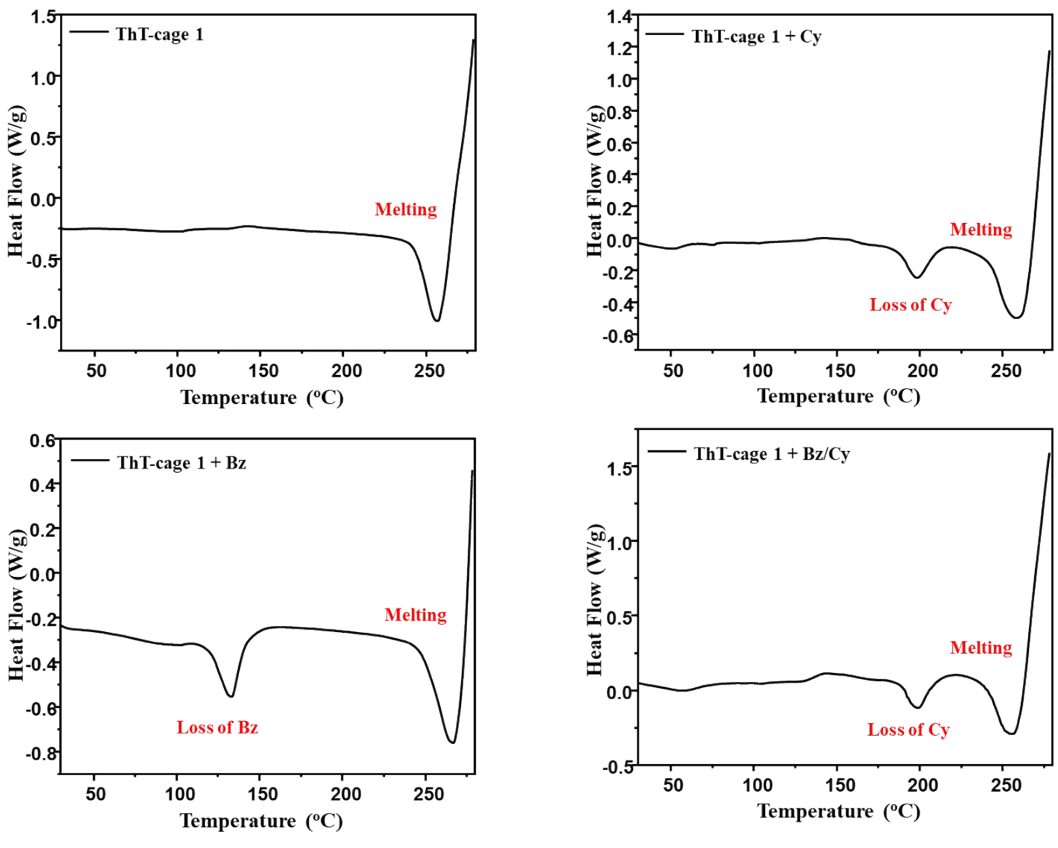

Fig. S16 Differential Scanning Calorimetry (DSC) of the **ThT-cage 1α** after being exposed to Bz/Cy for 24 h.

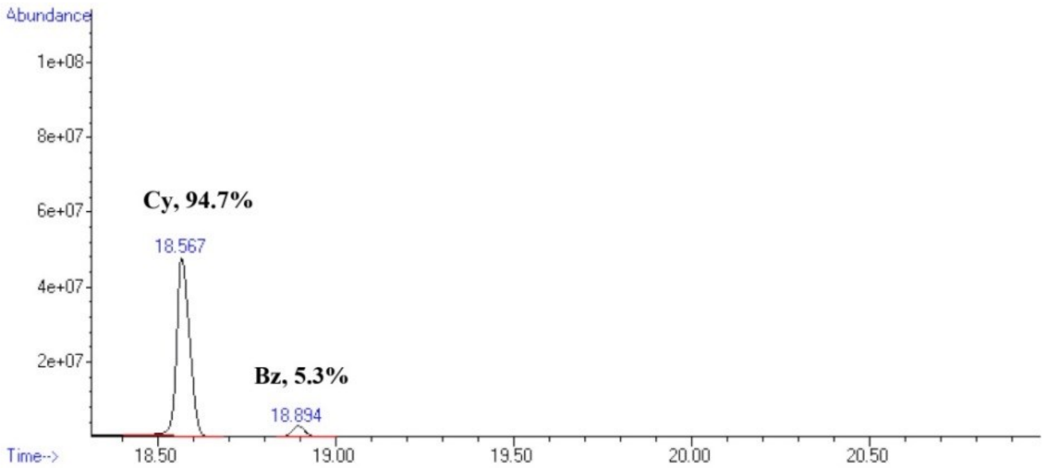

Fig. S17 Gas chromatography showing the relative uptake of Bz and Cy adsorbed by the **ThT-cage 1α** for 12h.

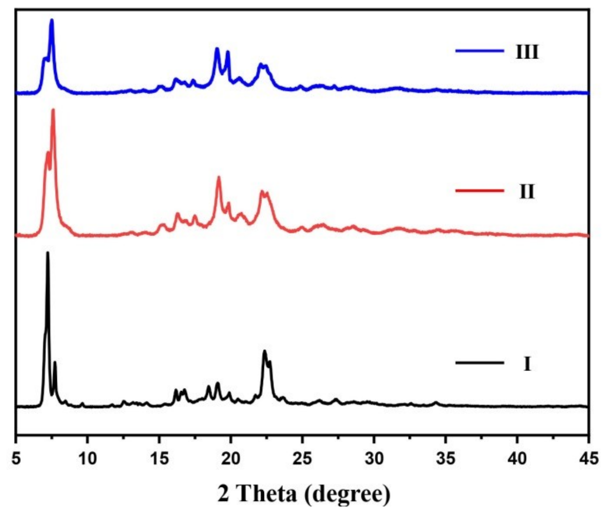

Fig. S18 Experimental PXRD patterns of the **ThT-cage 1α**: (Ⅰ) Original; (Ⅱ) Activated at 100 °C under vacuum after adsorption of Bz/Cy mixture vapor; (Ⅲ) Re-activated after 5 cycles.

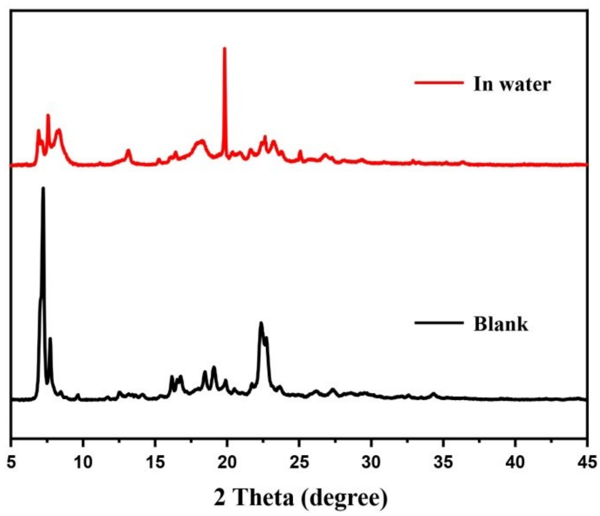

Fig. S19 Stability of the **ThT-cage 1α** in water for a week.

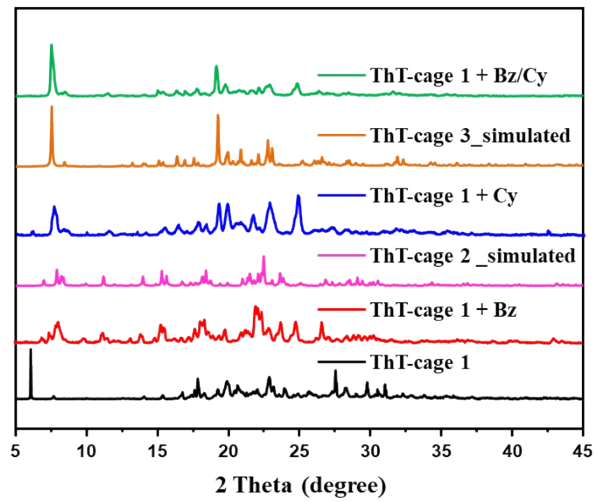

Fig. S20 Experimental PXRD patterns of crystal **ThT-cage 1** (with $CHCl_3$) after being soaked in Bz, Cy and Bz/Cy mixture solution for 24h.

Table S1. Experimental single crystal X-ray data

Identification code	**ThT-cage 1**	**ThT-cage 2**	**ThT-cage 3**
Empirical formula	$C_{38}H_{38}Cl_6N_8S_6$[a]	$C_{45}H_{45}N_8S_6$[a]	$C_{84}H_{96}N_{16}S_{12}$[a]
Formula weight	1011.82	890.25	1714.48
Temperature /K	150(2)	150(2)	120.72
Crystal system	Triclinic	Monoclinic	Orthorhombic
Space group	*P -1*	$P\ 2_1/n$	$P\ ca2_1$
a /Å	10.2559(3)	12.8314(3)	14.1011(9)
b /Å	15.7584(5)	15.7916(3)	14.1412(8)
c /Å	16.1989(6)	21.1780(5)	41.847(3)
α /°	67.5340(10)	90.00	90.00
β /°	71.5600(10)	92.5170(10)	90.00
γ /°	75.7500(10)	90.00	90.00
Volume /Å^3	2271.55(13)	4287.12(16)	8344.5(9)
Z	2	4	4
ρ_{calc} g/cm^3	1.479	1.379	1.365
μ /mm^{-1}	6.347	3.292	3.357
F(000)	1040	1868	3616
Radiation	CuKα (λ = 1.54178 Å)	CuKα (λ = 1.54178 Å)	CuKα (λ = 1.54178 Å)
Theta range for data collection/°	3.047 to 72.066	3.492 to 66.594	2.111 to 62.492
Index ranges	$-12\leq h\leq 12$, $-19\leq k\leq 19$, $-12\leq l\leq 19$	$-15\leq h\leq 15$, $-18\leq k\leq 18$, $-25\leq l\leq 25$	$-15\leq h\leq 16$, $-16\leq k\leq 14$, $-48\leq l\leq 48$
Reflections collected	77292	62287	66061
Independent reflections	8895 [R_{int} = 0.0378, R_{sigma} = 0.0185]	7303 [R_{int} = 0.0467, R_{sigma} = 0.0234]	12999 [R_{int} = 0.1155, R_{sigma} = 0.0869]
Data/restraints/parameters	8257/0 /523	6166/0 /532	10880/73 /1009
Goodness-of-fit on F^2	1.064	1.045	1.027
Final R indexes [I>=2σ (I)][b]	R_1 = 0.0505, wR_2 = 0.1390	R_1 = 0.0341, wR_2 = 0.0693	R_1 = 0.0699, wR_2 = 0.1598
Final R indexes [all data][b]	R_1 = 0.0533, wR_2 = 0.1418	R_1 = 0.0441, wR_2 = 0.0758	R_1 = 0.0839, wR_2 = 0.1666
CCDC	2058343	2058344	2058345

[a] Formula is given based on single-crystal X-ray data.

[b] $R_1 = \Sigma||F_o| - |F_c||/ \Sigma|F_o|$, $wR_2 = \{ \Sigma[w(F_o^2-F_c^2)^2]/ \Sigma[w(F_o^2)^2]\}^{½}$

Table S2. C-H···π intermolecular interactions between the aliphatic C-H moiety of TREN and centroid of the aromatic ring of Bz for **ThT-cage 2** crystals.

Distance	D–H···i (Å)	H···i (Å)	>D–H···i (°)
C5-H5B···π (C5···i1)	3.859	2.869	160.20

Table S3. C-H···S intermolecular interactions between the host and the guest molecules for **ThT-cage 2** crystals.

Distance	D–H···i (Å)	H···i (Å)	>D–H···i (°)
C39-H39···S1	3.799	2.849	176.48
C42-H42···S2	4.046	3.096	162.93

Table S4. C-H···N intermolecular interactions between cages for **ThT-cage 2** crystals.

Distance	D–H···i (Å)	H···i (Å)	>D–H···i (°)
C6A-H6A···N3	3.676	2.686	158.02
C15-H15B···N8	3.885	2.895	149.47

Table S5. Intermolecular π-π interactions distance between cages for **ThT-cage 2** crystals.

Distance	π···π (Å)
(i3···i4)	3.578

Table S6. C–H···S intermolecular interactions between the host and the guest molecules for **ThT-cage 3** crystals.

Distance	D–H···i (Å)	H···i (Å)	>D–H···i (°)
C63-H63A···S11	3.933	2.943	140.83
C77-H77A···S4	3.867	2.877	146.27
C78-H78B···S12	4.027	3.037	140.76
C82-H82A···S10	3.914	2.924	140.83

Table S7. C-H···π intermolecular interactions between the aliphatic C-H of the cyclohexane ring and the centroid of the 5-membered ring of the cage for **ThT-cage 3** crystals.

Distance	D–H···i (Å)	H···i (Å)	>D–H···i (°)
C72-H72A···π (C72···i2)	3.761	2.771	141.54
C75-H75B···π (C75···i3)	3.684	2.694	149.81

Table S8. C-H···N hydrogen bonding interactions between the cages for **ThT-cage 3** crystals.

Distance	D–H···i (Å)	H···i (Å)	>D–H···i (°)
C33-H33A···N5	3.501	2.511	152.71
C42-H42A···N13	3.756	2.766	158.14
C44-H44B···N3	3.526	2.536	150.32
C51-H51B···N11	3.660	2.670	129.32
C62-H62A···N16	3.667	2.677	163.31
C65-H65A···N8	3.952	2.962	147.60

Table S9. Optimized Structures and Binding Energies of the THT-cage with Bz or Cy.

THT-cage	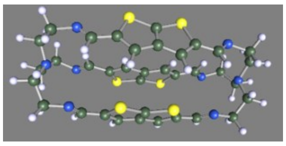	**3D Structure: THT-cage + Solvent**	**Binding Energy at 1 bar and 298.15 K**
Bz	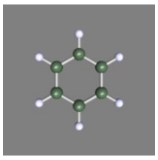	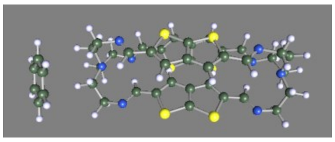	ΔG_{gas} (kcal·mol^{-1}) = -7.742 ΔG_{water} (kcal·mol^{-1}) = -5.159
Cy	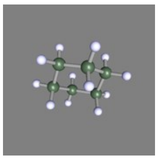	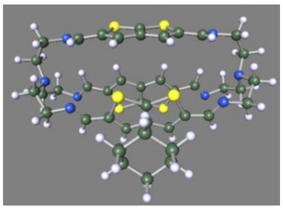	ΔG_{gas} (kcal·mol^{-1}) = -11.50 ΔG_{water} (kcal·mol^{-1}) = -8.350

The structure of each studied molecule (i.e., THT-cage alone and with Bz or Cy) was optimized by using the Turbomole 7.0 program package.[5] Before their visualization using TmoleX (version 4.1.1), the structure of each individual species (i.e. THT-cage, Bz and Cy) was optimized in the gas phase, with a convergence criterion of 10-8 Hartree, using the hybrid functional UB3LYP and the triplet-ζ basis set 6-311+G*,[6] to collect its more stable 3D conformer. The resulting optimized structure was then used as an input in the COSMOconfX program (version 4.0) to generate the lowest energy contact between the THT-cage and Bz or Cy to form each cluster (i.e., THT-S with S = Bz or Cy).

The energy of each cluster (THT-S) was then minimized again using DFT calculations combining the Resolution of Identity (RI) approximation,[7-8] within the Turbomole 7.0 program package using the UB3LYP function with the def2-TZVP basis set.[9-11] All major trends obtained with the UB3LYP functional were replicated with the pure UBP86 function. All minimum energy structures were obtained with full optimization, without constraints. Corrections for long range non-bonding interactions were given using the Grimme D3 dispersion model.[12] An implicit solvent model of water was additionally undertaken, using the COSMO Model implemented in Turbomole. Analytical frequencies were conducted on each structure at 1 atm and 298.15 K to calculate each binding energy when mixing THT-cage with Bz or Cy.

Table S10. Summary of the selective adsorbents for the separation of Bz and Cy.

Adsorbents	Nature of adsorbent	Temp. (K)	Selective uptake (Bz/Cy)	Selective uptake (Cy/Bz)	Reference
TCNQ-based PCPs	Hybrid	298 K	96 : 4 (Vap.)	-	13
TCNQ-based PCPs	Hybrid	298 K	90 : 10 (Vap.)	-	14
MOF 1	Hybrid	298 K	92 : 1 (Liq.)	-	15
MOF 1	Hybrid	298 K	20 : 1 (Vap.)	-	15
Hybrid[3]arene	Organic	298 K	97.5 : 2.5 (Vap.)	-	16
Tiara[5]arene	Organic	298 K	92.3 : 7.7 (Vap.)	-	118
Naphthotubes	Organic	298 K	90.7 : 9.3 (Vap.)	-	10
Thienothiophene -based cages	Organic	298 K	-	94 : 6 (Vap.)	Our Work

References

[1] SAINT. Bruker AXS. Inc, Madison, Wisconsin, USA, 2014.

[2] SADABS. G. M. Sheldrick, University of Gottingen, Germany, 2008.

[3] G. M. Sheldrick, A Short History of SHELX. *Acta Crystallogr.* 2008, **A64**, 112 -122.

[4] L. J. Barbour, *Supramol. Chem.* 2001, **1**,189 –191.

[5] R. Ahlrichs, M. Bär, M. Häser, H. Horn, C. Kölmel, *Chem. Phys. Lett.* 1989, **162**, 165-169.

[6] C. A. Jiménez-Hoyos, B. G. Janesko, G. E. Scuseria, *Phys. Chem. Chem. Phys.* 2008, **10**, 6621-6629.

[7] F. Weigend, M. Häser, *Theor. Chem. Acc.* 1997, **97**, 331-340.

[8] F. Weigend, M. Häser, H. Patzelt, R. Ahlrichs, *Chem. Phys. Lett.* 1998, **294**, 143-152.

[9] A.D. Becke, *Phys. Rev. A* 1988, **38**, 3098-3100.

[10] C. Lee, W. Yang, R.G. Parr, *Phys. Rev. B* 1988, **37**, 785-789.

[11] S. Grimme, *J. Comput. Chem.* 2006, **27**, 1787-1799.

[12] S. Grimme, J. Antony, S. Ehrlich,H. A. Krieg, *J. Chem. Phys.* 2010, **132**, 154104.

[13] S. Shimomura, S. Horike, R. Matsuda, S. Kitagawa, *J. Am. Chem. Soc.* 2007, **129**, 10990-10991.

[14] S. Shimomura, R. Matsuda, S. Kitagawa, *Chem. Mater.* 2010, **22**, 4129-4131.

[15] A. A. Lysova, D. G. Samsonenko, P, V. Dorovatovskii, V. A. Lazarenko, V. N. Khrustalev, K. A. Kovalenko, D. N. Dybtsev, V. P. Fedin, *J. Am. Chem. Soc.* 2019, **141**, 17260-17269.

[16] J. Zhou, G. Yu, Q. Li, M. Wang, F. Huang, *J. Am. Chem. Soc.* 2020, **142**, 2228-2232.

[17] W. Yang, K. Samanta, X. Wan, T. U. Thikekar, Y. Chao, S. Li, K. Du, J. Xu, Y. Gao, H. Zuihof, A. C. H. *Angew. Chem. Int. Ed.* 2020, **59**, 3994-3999.

[18] H. Yao, Y. M. Wang, M. Quan, M. U. Farooq, L. P. Yang, W. Jiang, *Angew. Chem. Int. Ed.* 2020, **59**, 19945-19950.